Supplement to The 1-way on-line coupled model system MECO(n) – Part 4: Chemical evaluation (based on MESSy v2.52)

Mariano Mertens
Institut für Physik der Atmosphäre
DLR-Oberpfaffenhofen

mariano.mertens@dlr.de

December 2015

Contents

S1 Supplementary figures

S1.1 Dry deposition rates

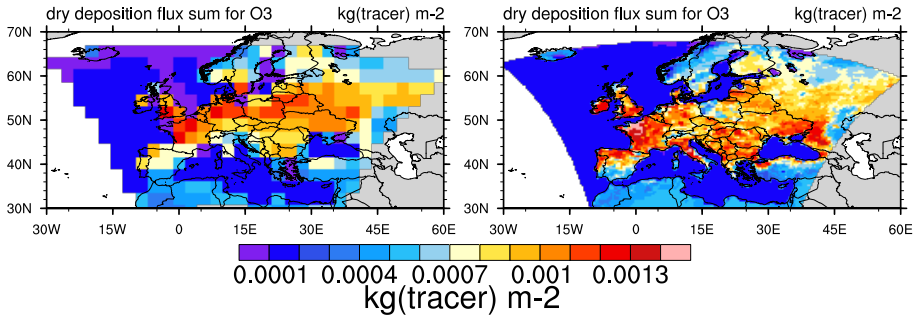

Figure S1: Dry deposition sum for June 2008 of ozone (in kg m^{-2}) from EMAC (left) and COSMO (right). Over Poland less ozone is deposited in COSMO compared to EMAC. This is due to different soil types in both models.

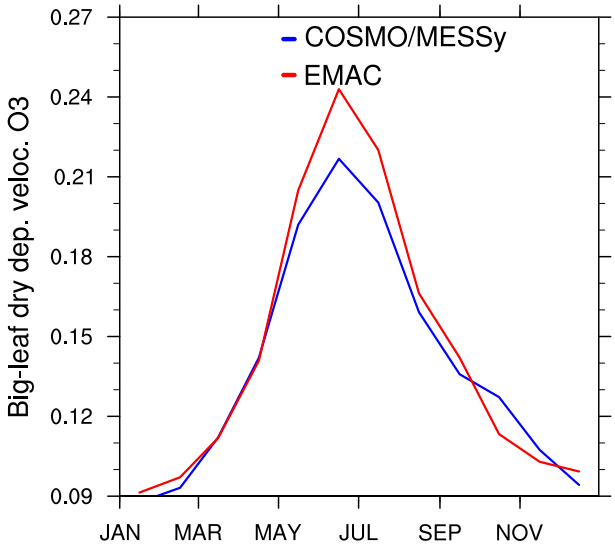

Figure S2: Monthly area weighted average dry deposition flux velocity (in cm s^{-1}) for EMAC and COSMO.

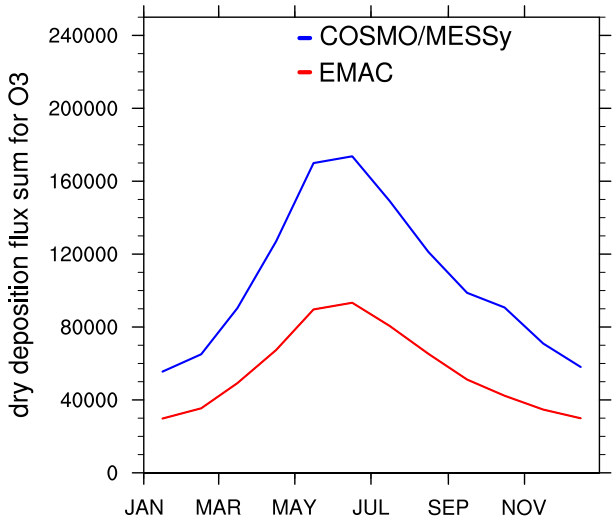

Figure S3: Monthly averaged dry deposition flux (in kg O_3) from EMAC and COSMO.

S1.2 On-line calculated emissions of soil-NO_x and isoprene

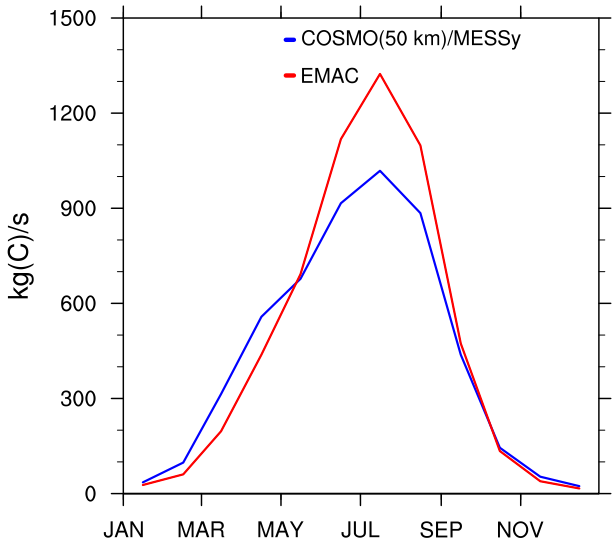

Figure S4: Monthly averaged on-line emissions of isoprene (in kg(C) s^{-1}). The emissions are summed over all gridboxes within the domain of the COSMO(50km)/MESSy instance (neglecting the relaxation area). Please note, that the unscaled emissions are plotted.

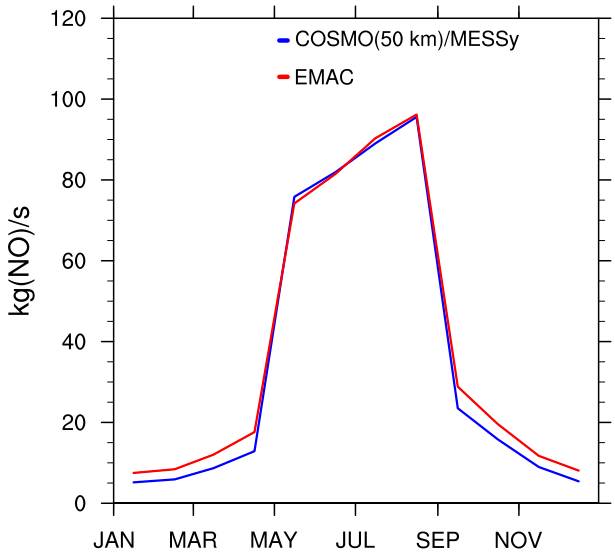

Figure S5: Monthly averaged on-line emissions of soil-NO_x (in kg(NO) s^{-1}). The emissions are summed over all gridboxes within the domain of the COSMO(50km)/MESSy instance (neglecting the relaxation area). The increase of the emissions in the period from May - August are mainly due to the fact, that the algorithm assumes increased fertilization of agricultural areas in this period.

S1.3 Annual cycle of ozone at different stations

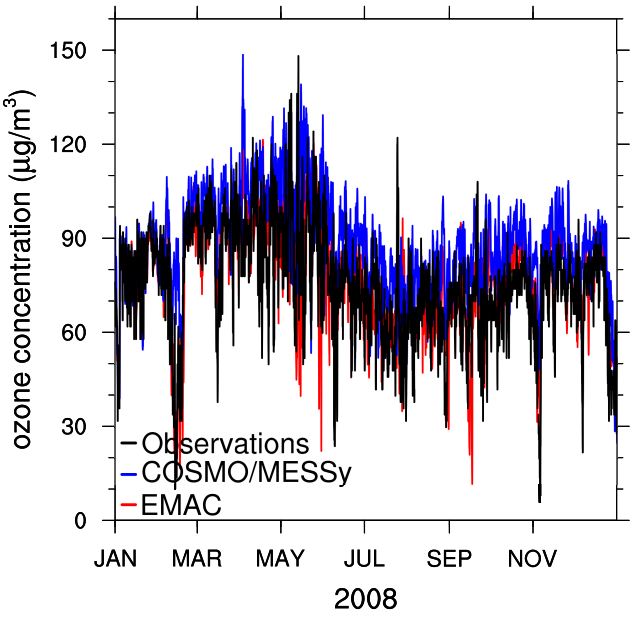

Figure S6: Box-smoothed (7 days) average of ozone concentration (observed and simulated) at the Mace Head station in Ireland.

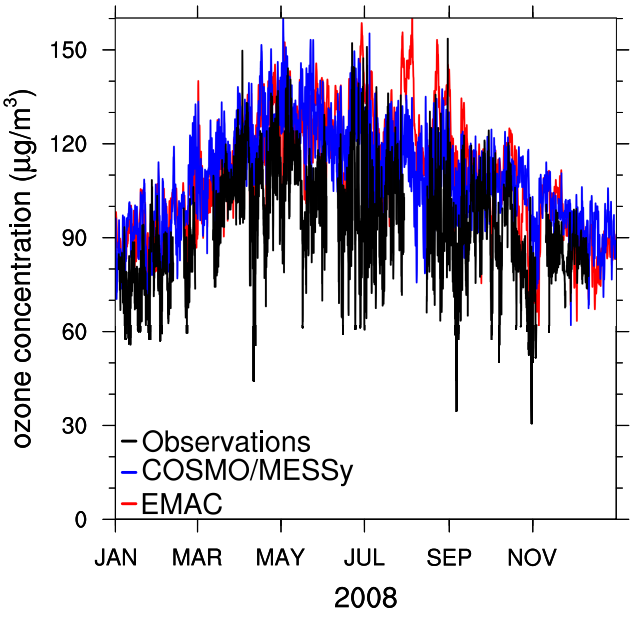

Figure S7: As Fig. S6 but for Giordan Lighthouse, Malta.

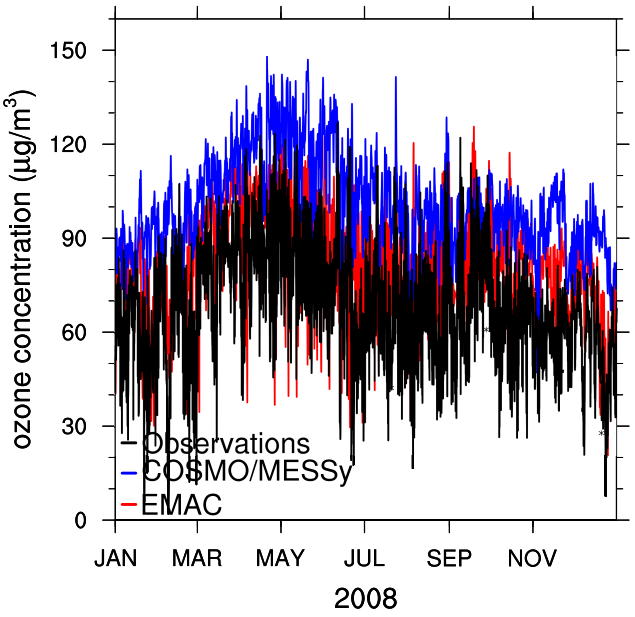

Figure S8: As Fig. S6 but for Niembro, Spain.

S1.4 Taylor diagrams with non 'height corrected' results

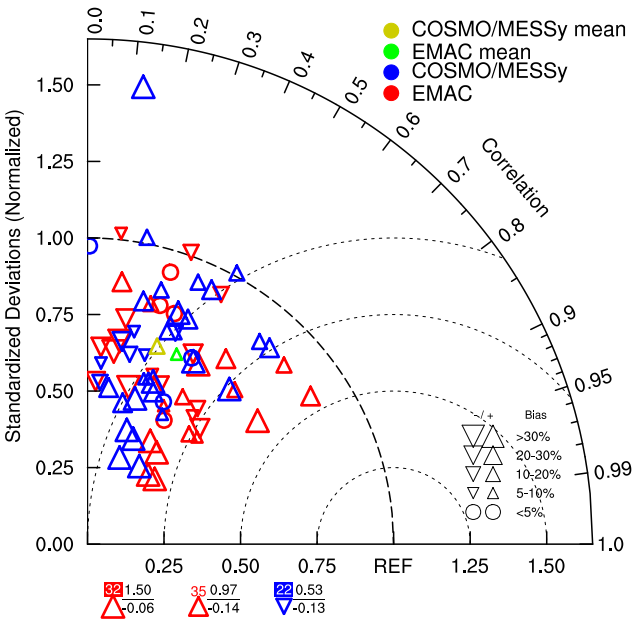

Figure S9: Taylor diagram for ground level ozone concentrations in June 2008. The results for EMAC are indicated in red, for COSMO/MESSy in blue. The mean over all stations is coloured in green for EMAC and in golden colour for COSMO/MESSy. The size of the symbols indicate the bias in percent; upward symbols show a positive bias, downward symbols a negative bias. In difference to the Taylor diagram in the main manuscript the non height corrected values are used here.

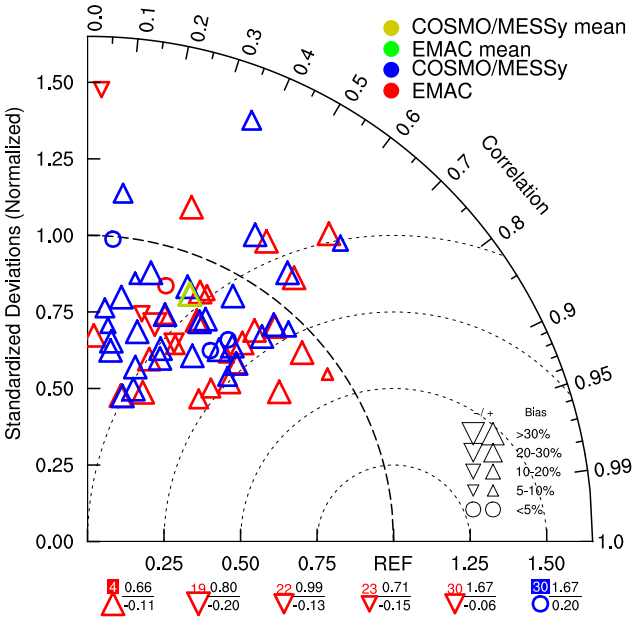

Figure S10: As Fig. S9 but for December 2008.

S1.5 Nitrogen dioxide concentrations for June 2008

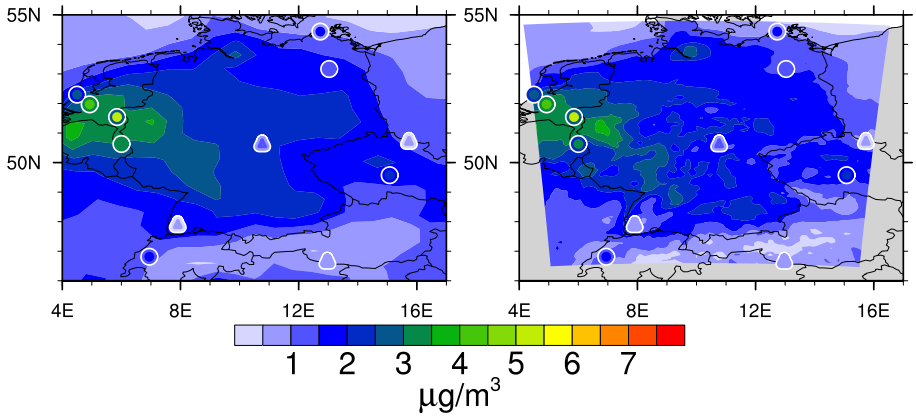

Figure S11: Monthly averaged nitrogen dioxide concentrations in µg (N) m^{-3} from COSMO(50km)/MESSy (left) and COSMO(12km)/MESSy (right) at the lowest model layer for June 2008. The inner part of the coloured dots depicts the monthly mean values measured at the corresponding stations, while the outer part shows the simulated value corrected for the station height.

S1.6 Nitric acid concentrations

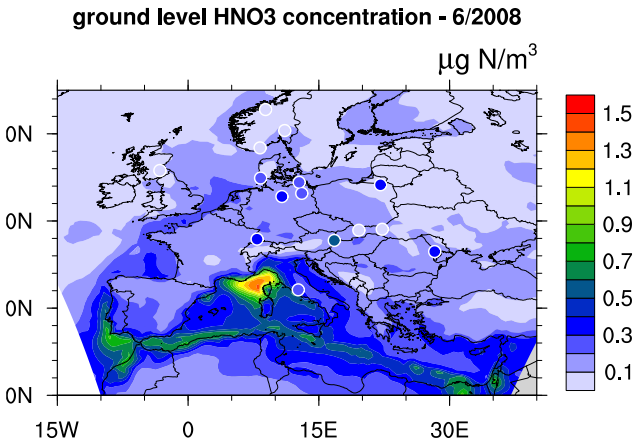

Figure S12: Monthly averaged nitric acid concentrations in µg (N) m^{-3} from COSMO(50km)/MESSy at the lowest model layer for June 2008. The coloured dots depicts the monthly mean values measured at the corresponding stations.

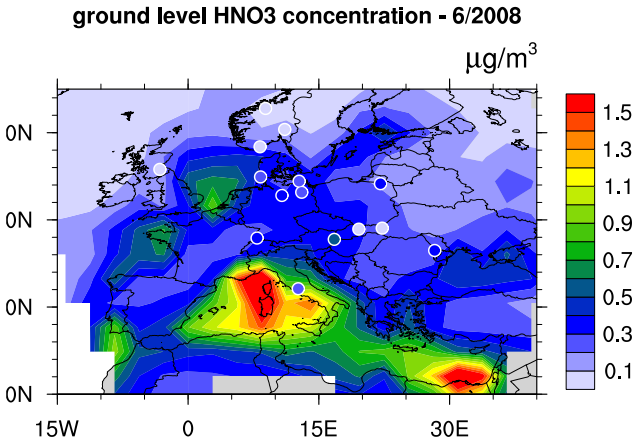

Figure S13: As figure S12 but for EMAC.

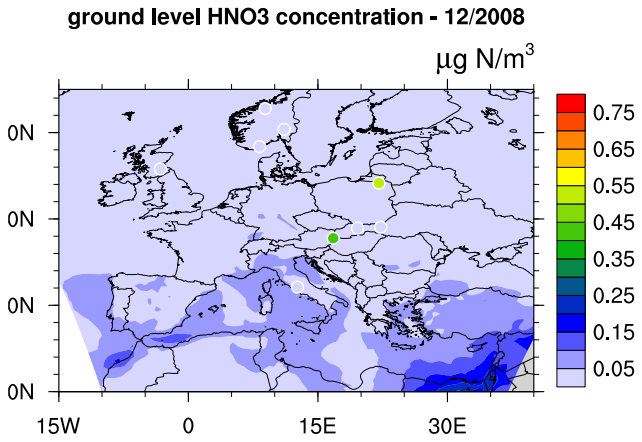

Figure S14: Monthly averaged nitric acid concentrations in µg (N) m^{-3} from COSMO(50km)/MESSy at the lowest model layer for December 2008. The coloured dots show the monthly mean values measured at the corresponding stations.

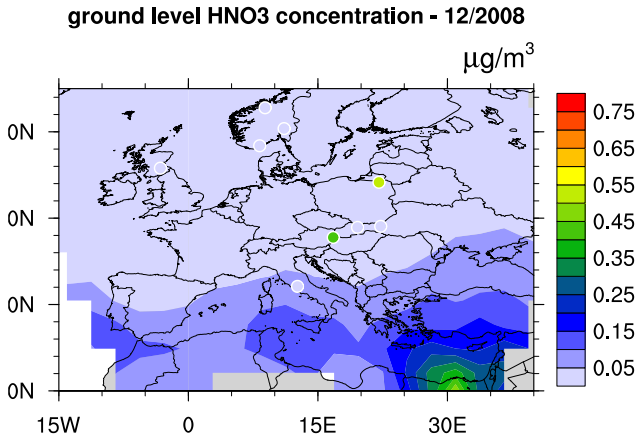

Figure S15: As Fig. S14 but for EMAC.

S1.7 Isoprene mixing ratios

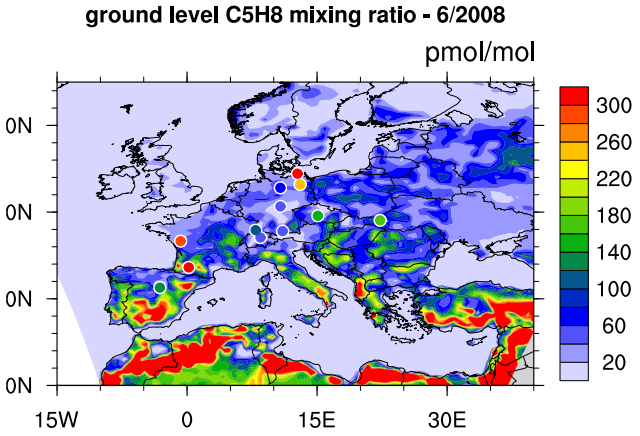

Figure S16: Monthly averaged isoprene mixing ratios in pmol mol^{-1} from COSMO(50km)/MESSy at the lowest model layer for June 2008. The coloured dots show the monthly mean values measured at the corresponding stations.

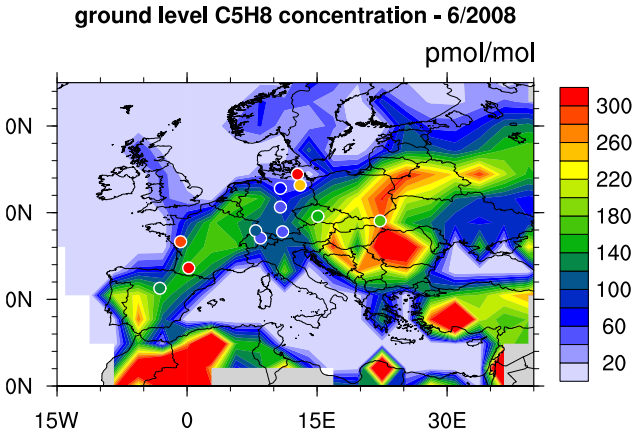

Figure S17: As Fig. S16 but for EMAC.

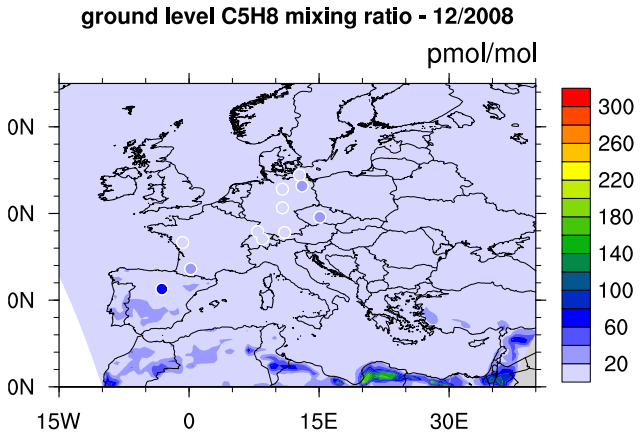

Figure S18: Monthly averaged isoprene mixing ratios in pmol mol^{-1} from COSMO(50km)/MESSy at the lowest model layer for June 2008. The coloured dots show the monthly mean values measured at the corresponding stations.

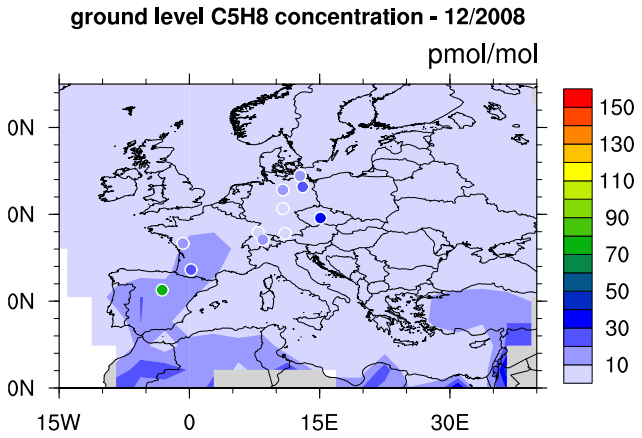

Figure S19: As Fig. S18 but from EMAC.

S1.8 Vertical ozone profiles

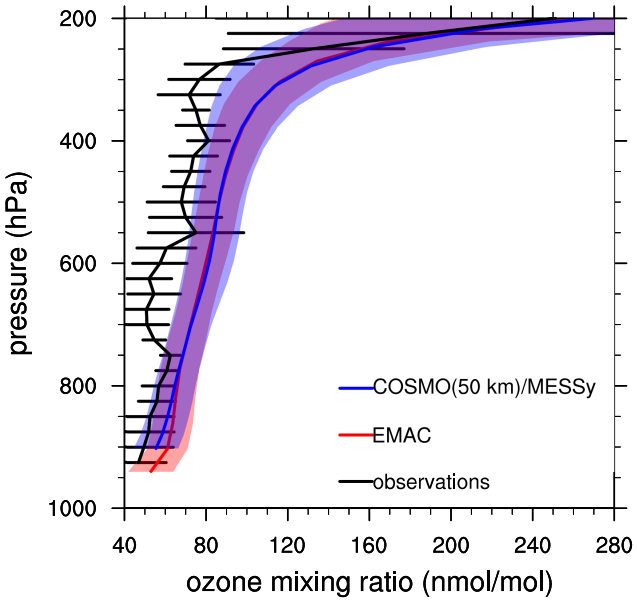

Figure S20: Vertical ozone profile at Madrid for June 2008. The standard deviation of the temporal mean is indicated by the error bars for the observations and by the shaded area for the model data.

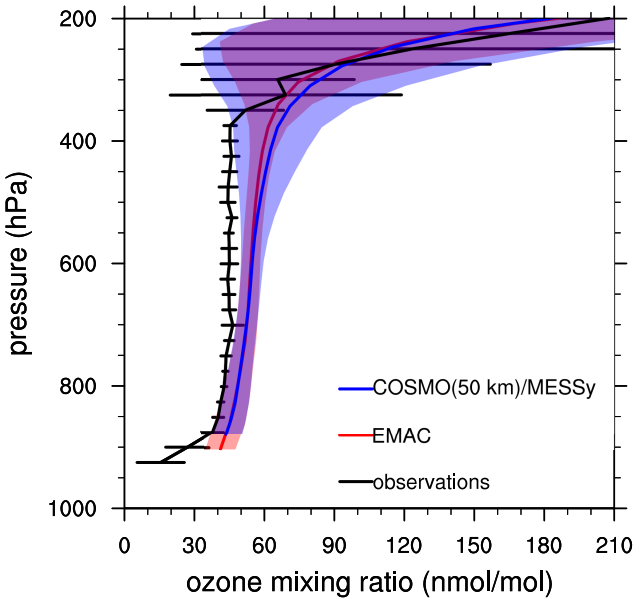

Figure S21: As Fig. S20 but for December 2008.

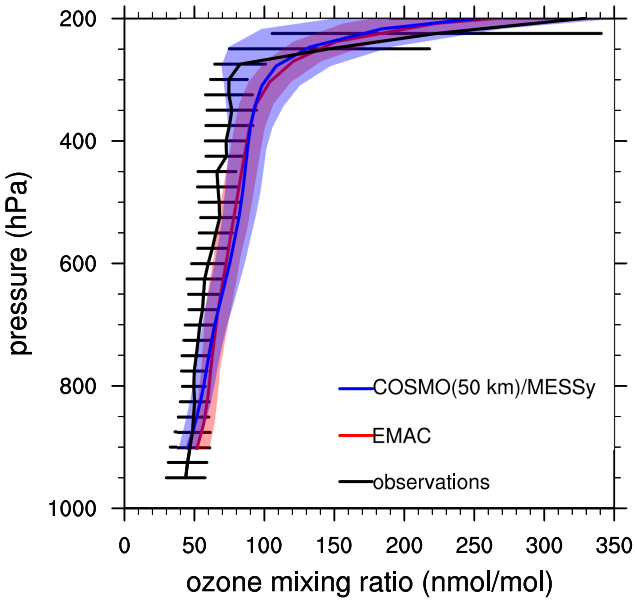

Figure S22: Vertical ozone profile at Payerne for June 2008. The standard deviation of the temporal mean is indicated by the error bars for the observations and by the shaded area for the model data.

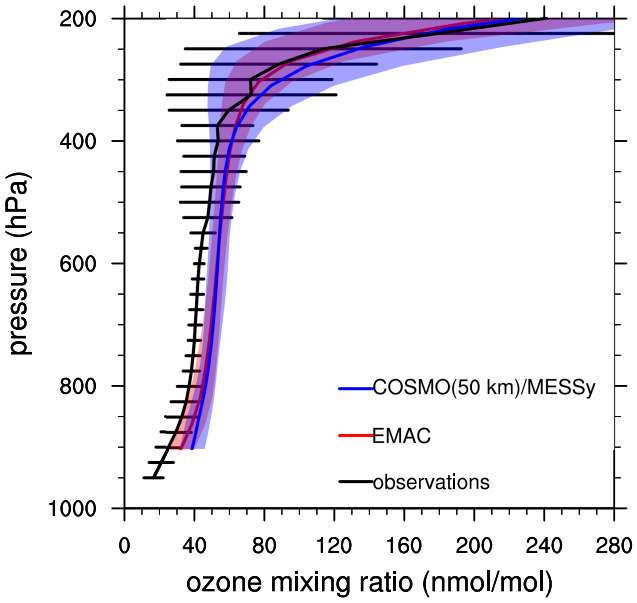

Figure S23: As Fig. S23 but for December 2008.

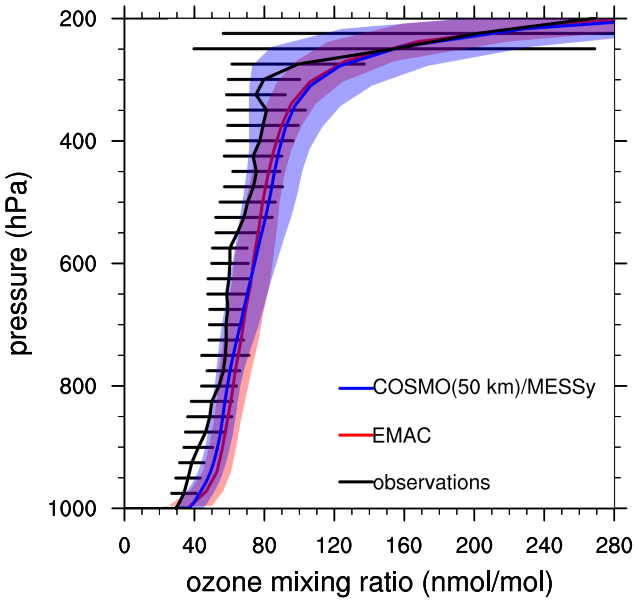

Figure S24: Vertical ozone profile at Uccle for June 2008. The standard deviation of the temporal mean is indicated by the error bars for the observations and by the shaded area for the model data.

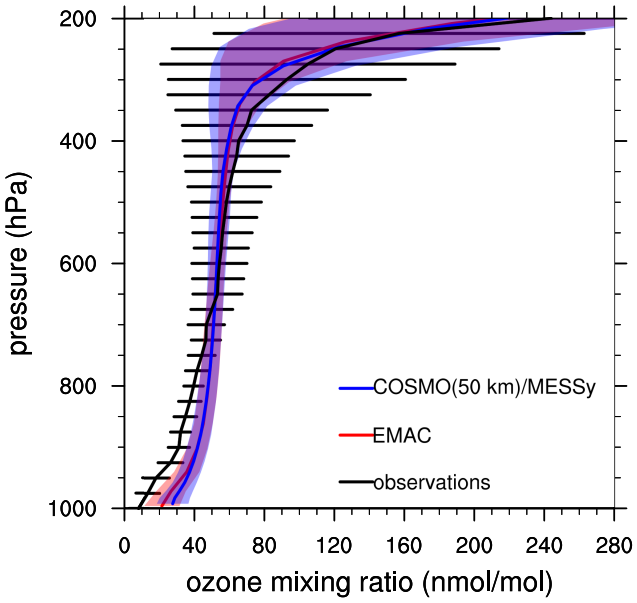

Figure S25: As Fig. S25 but for December 2008.

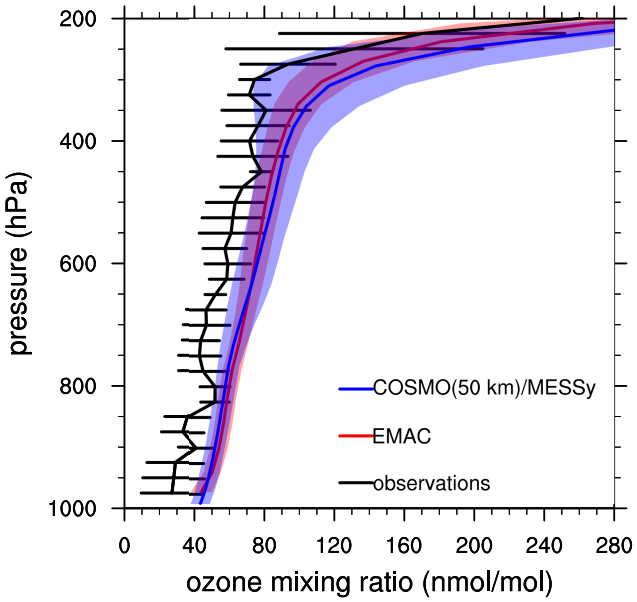

Figure S26: Vertical ozone profile at Legionowo for June 2008. The standard deviation of the temporal mean is indicated by the error bars for the observations and by the shaded area for the model data.

S2 Comparison with ERA-Interim

S2.1 COSMO(50km)/MESSy

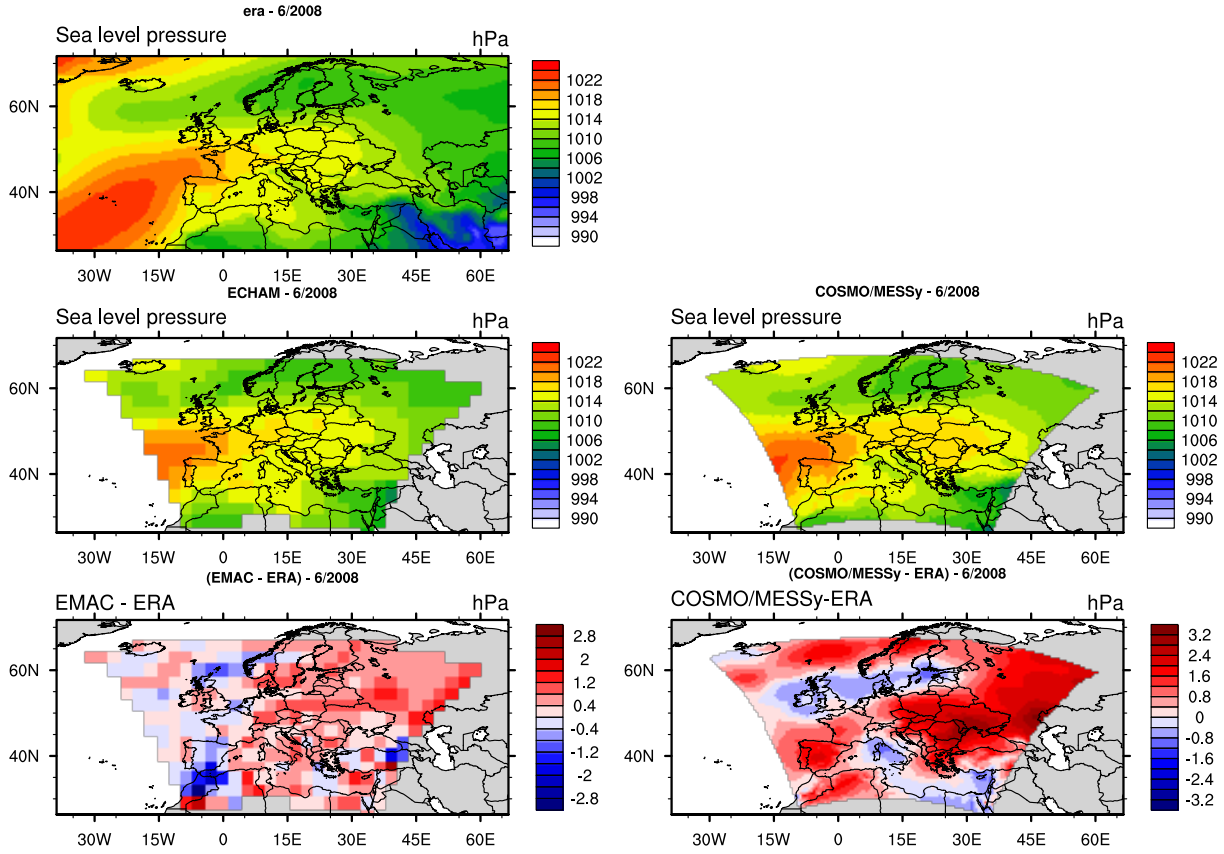

Figure S27: Comparison of the mean sea level pressure (in hPa) between EMAC, COSMO(50km)/MESSy and ERA Interim for June 2008. The upper three plots show the absolute values for ERA-Interim, EMAC and COSMO(50km)/MESSy. The lower row depicts the difference to ERA-Interim for EMAC (left) and COSMO(50km)/MESSy (right).

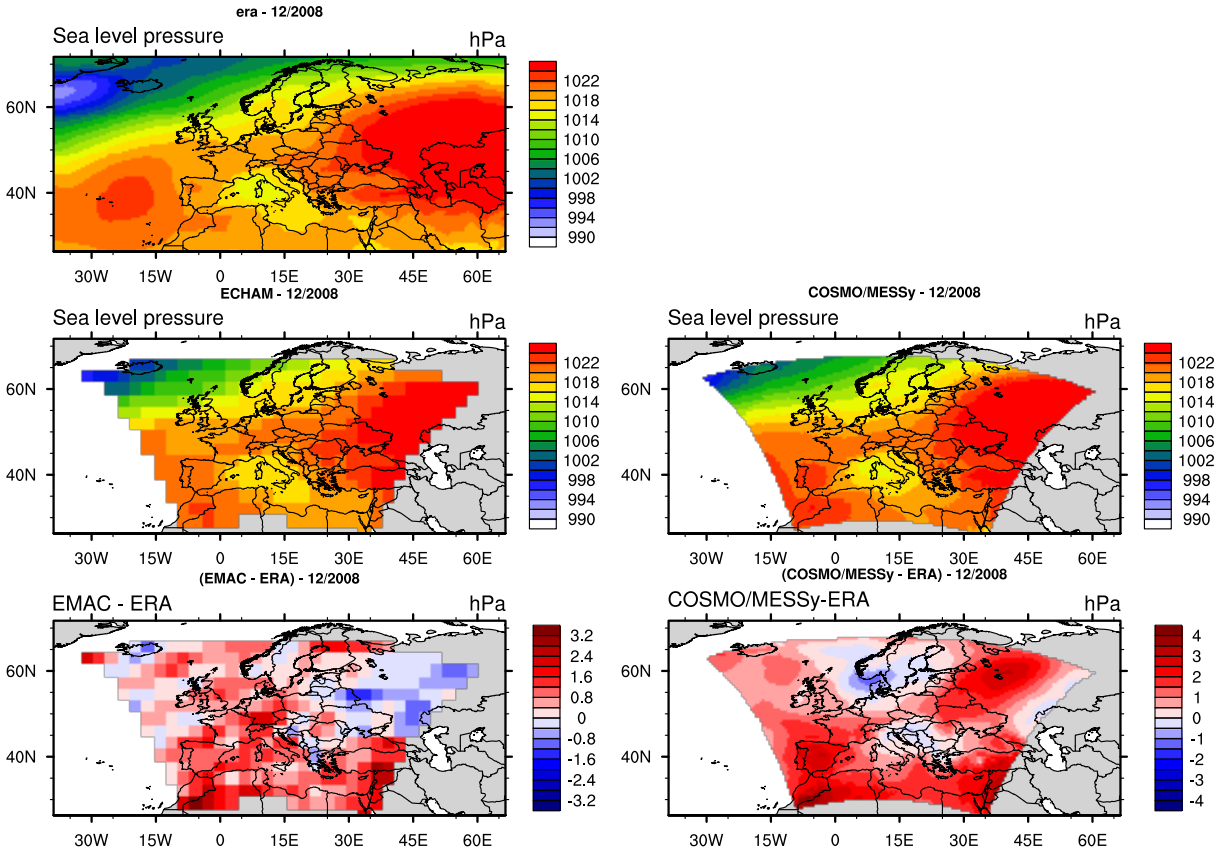

Figure S28: As Fig. S27 but for December 2008.

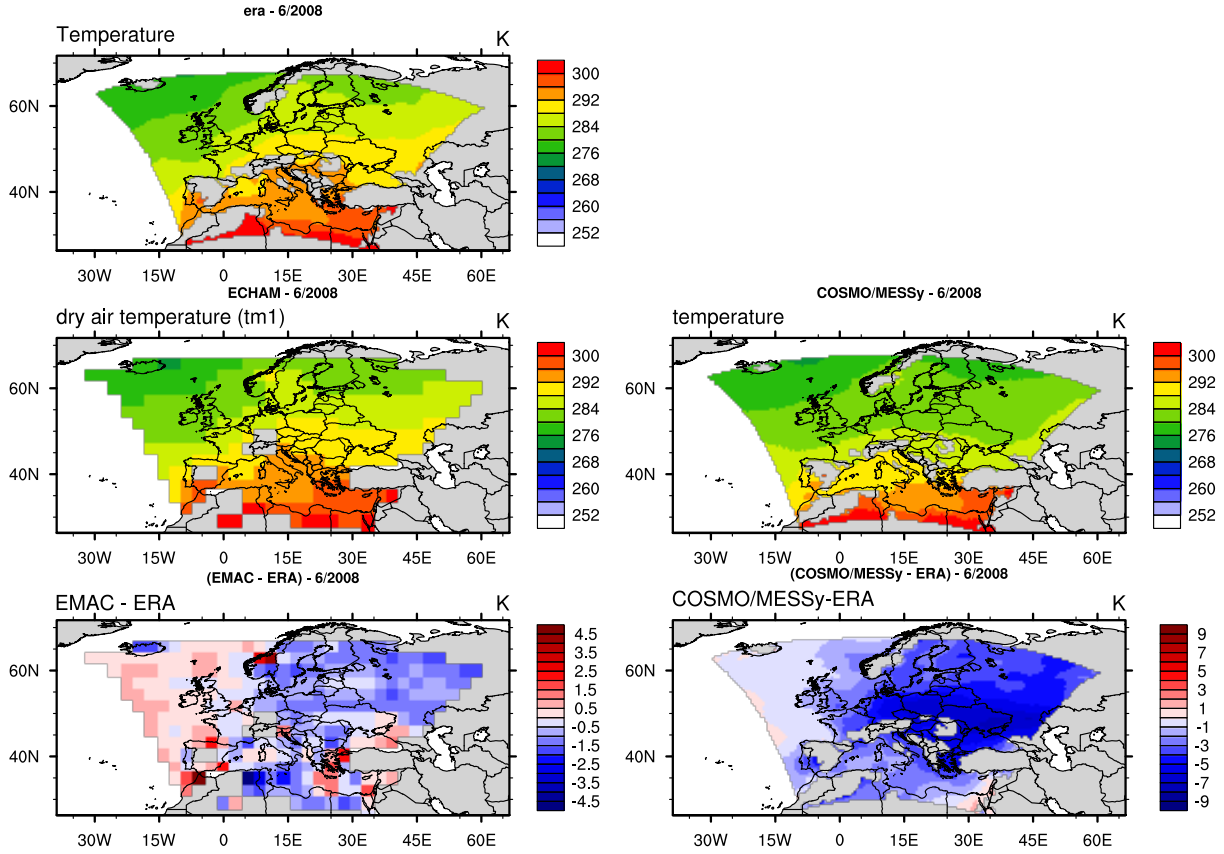

Figure S29: Comparison of the temperature at 950 hPa (in K) between EMAC, COSMO(50km)/MESSy and ERA Interim for June 2008. The upper three plots show the absolute values for ERA-Interim, EMAC and COSMO(50km)/MESSy. The lower row depicts the difference to ERA-Interim for EMAC (left) and COSMO(50km)/MESSy (right).

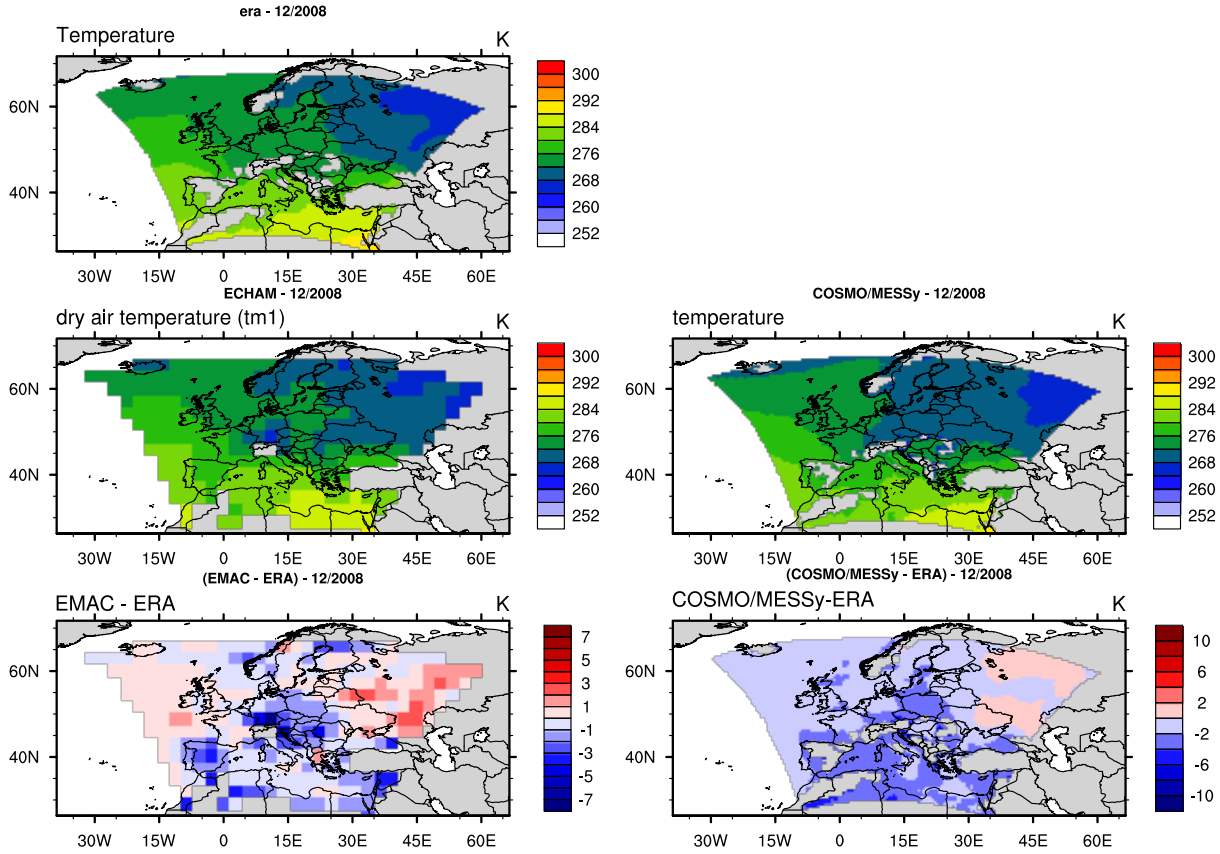

Figure S30: As Fig. S29 but for December 2008.

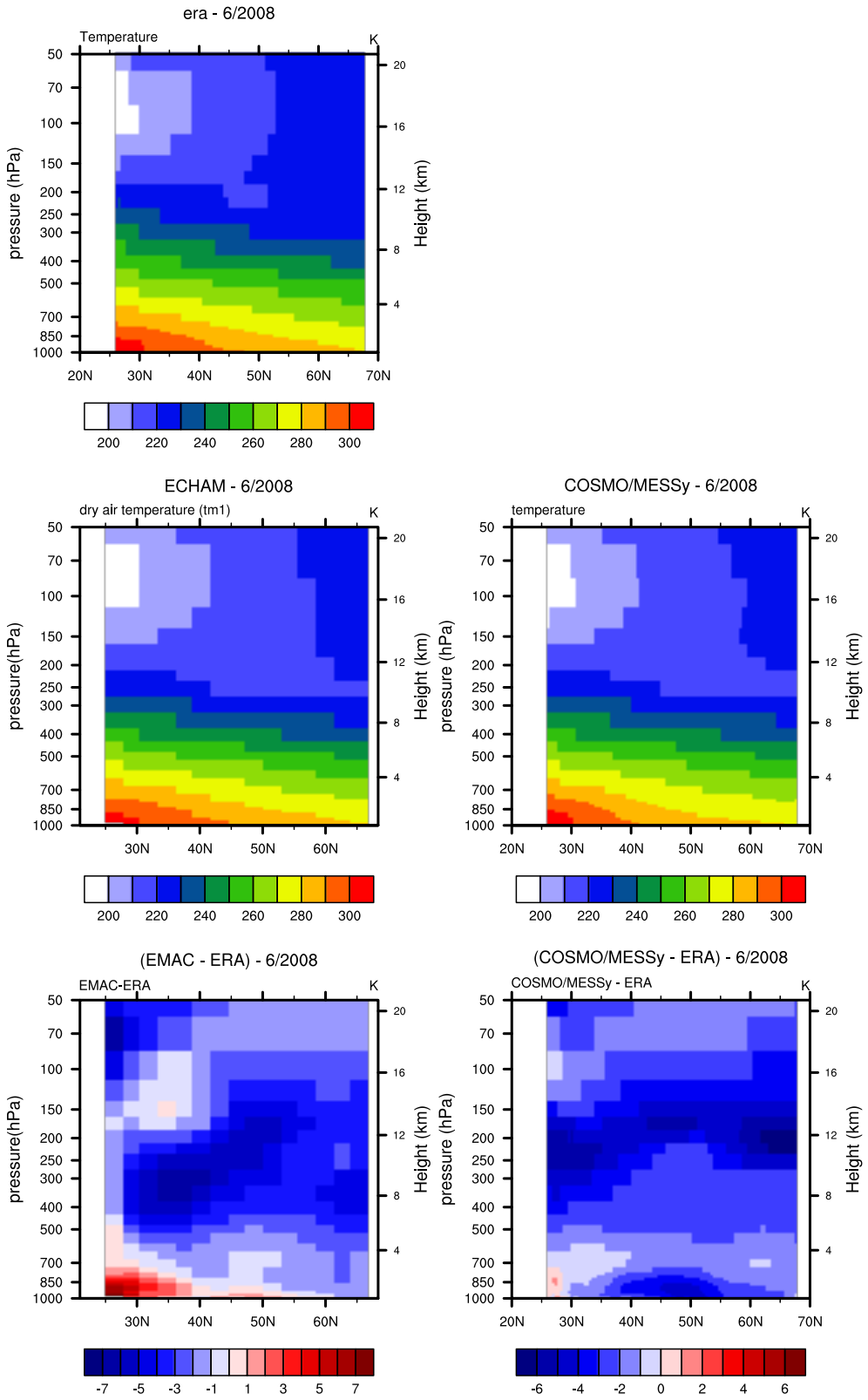

Figure S31: Comparison of the zonal average temperature (in K) between EMAC, COSMO(50km)/MESSy and ERA Interim for June 2008. The upper three plots show the absolute values for ERA-Interim, EMAC and COSMO(50km)/MESSy. The lower row depicts the difference to ERA-Interim for EMAC (left) and COSMO(50km)/MESSy (right).

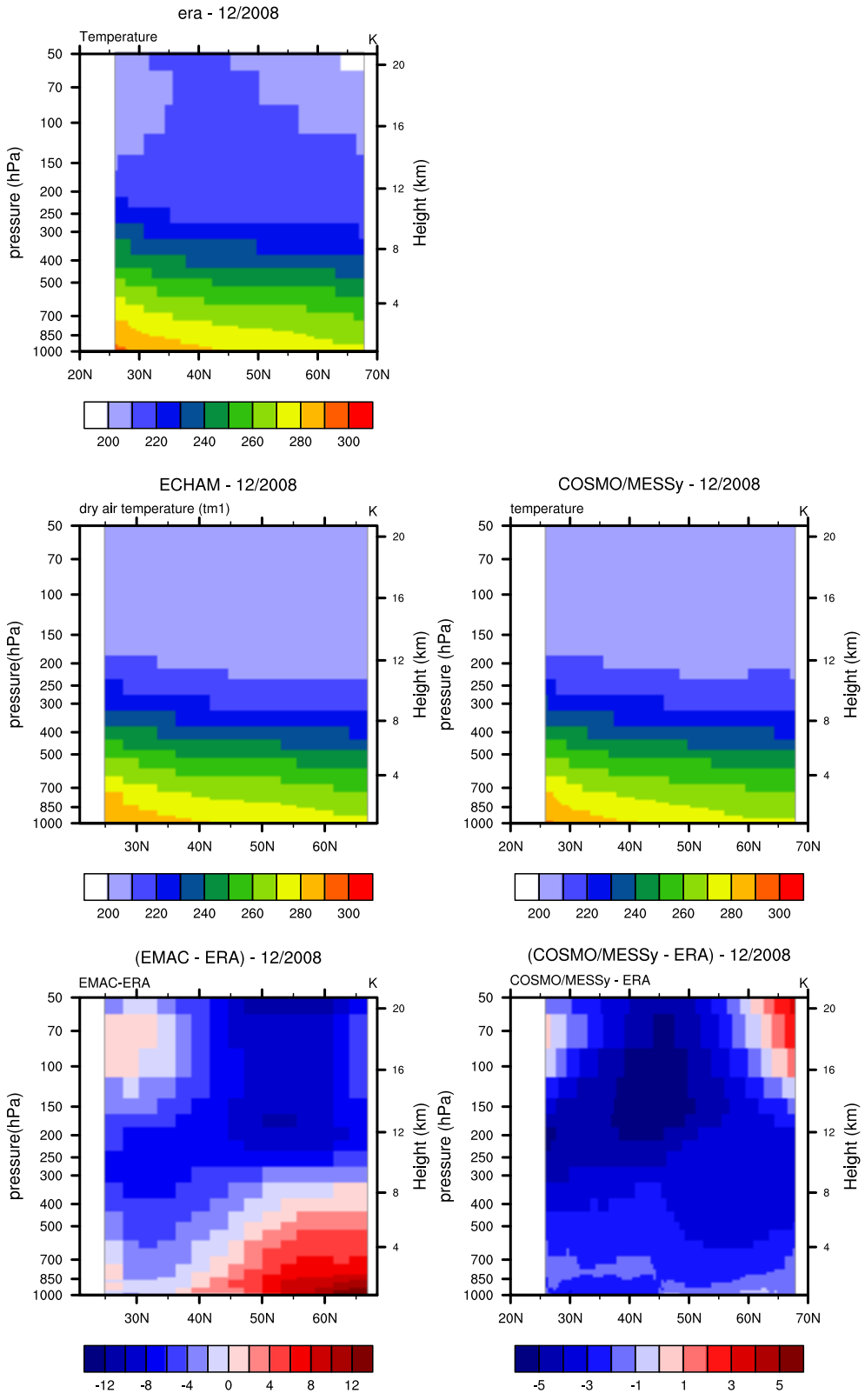

Figure S32: As Fig. S31 but for December 2008.

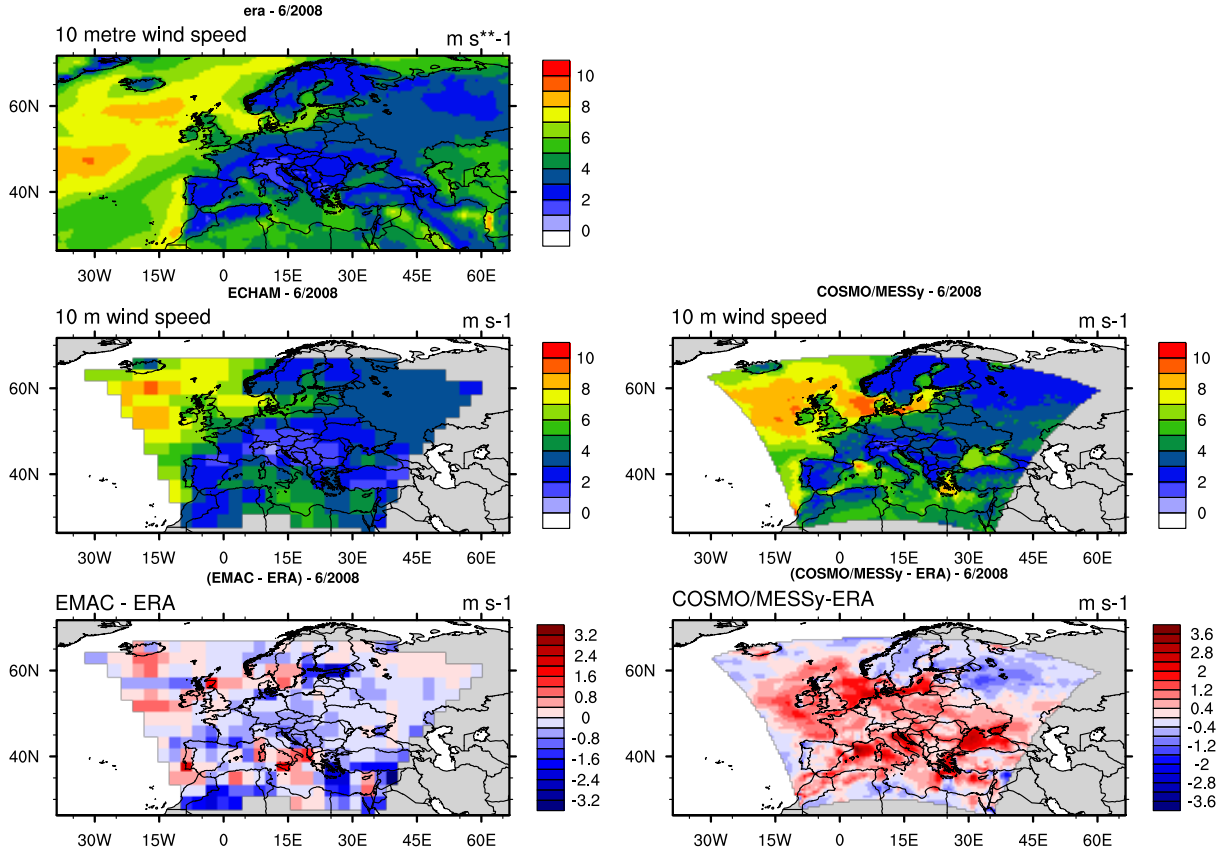

Figure S33: Comparison of the 10 meter wind speed (in $\mathrm{m\,s^{-1}}$) between EMAC, COSMO(50km)/MESSy and ERA Interim for June 2008. The upper three plots show the absolute values for ERA-Interim, EMAC and COSMO(50km)/MESSy. The lower row depicts the difference to ERA-Interim for EMAC (left) and COSMO(50km)/MESSy (right).

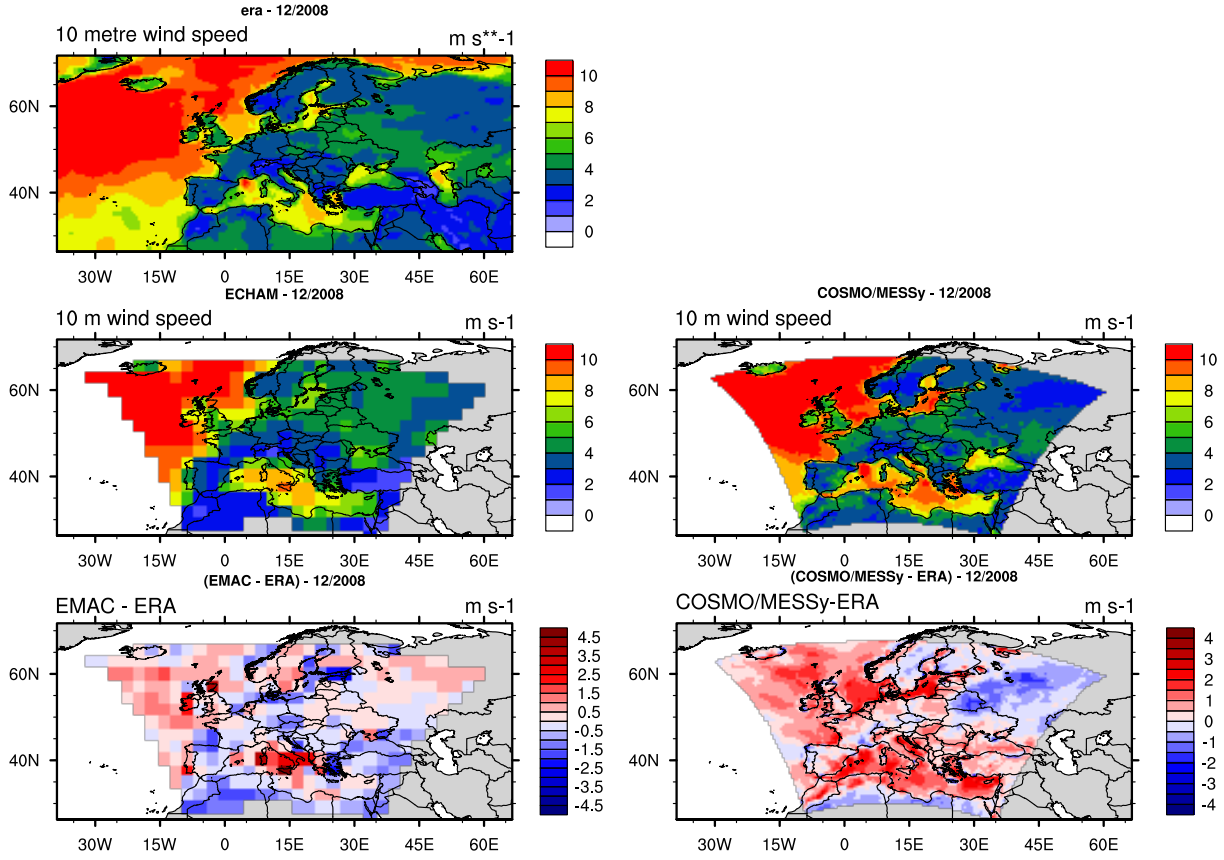

Figure S34: Comparison of the 10 meter wind speed (in m s^{-1}) between EMAC, COSMO(50km)/MESSy and ERA Interim for December 2008. The upper three plots show the absolute values for ERA-Interim, EMAC and COSMO(50km)/MESSy. The lower row depicts the difference to ERA-Interim for EMAC (left) and COSMO(50km)/MESSy (right).

S2.2 COSMO(12km)/MESSy

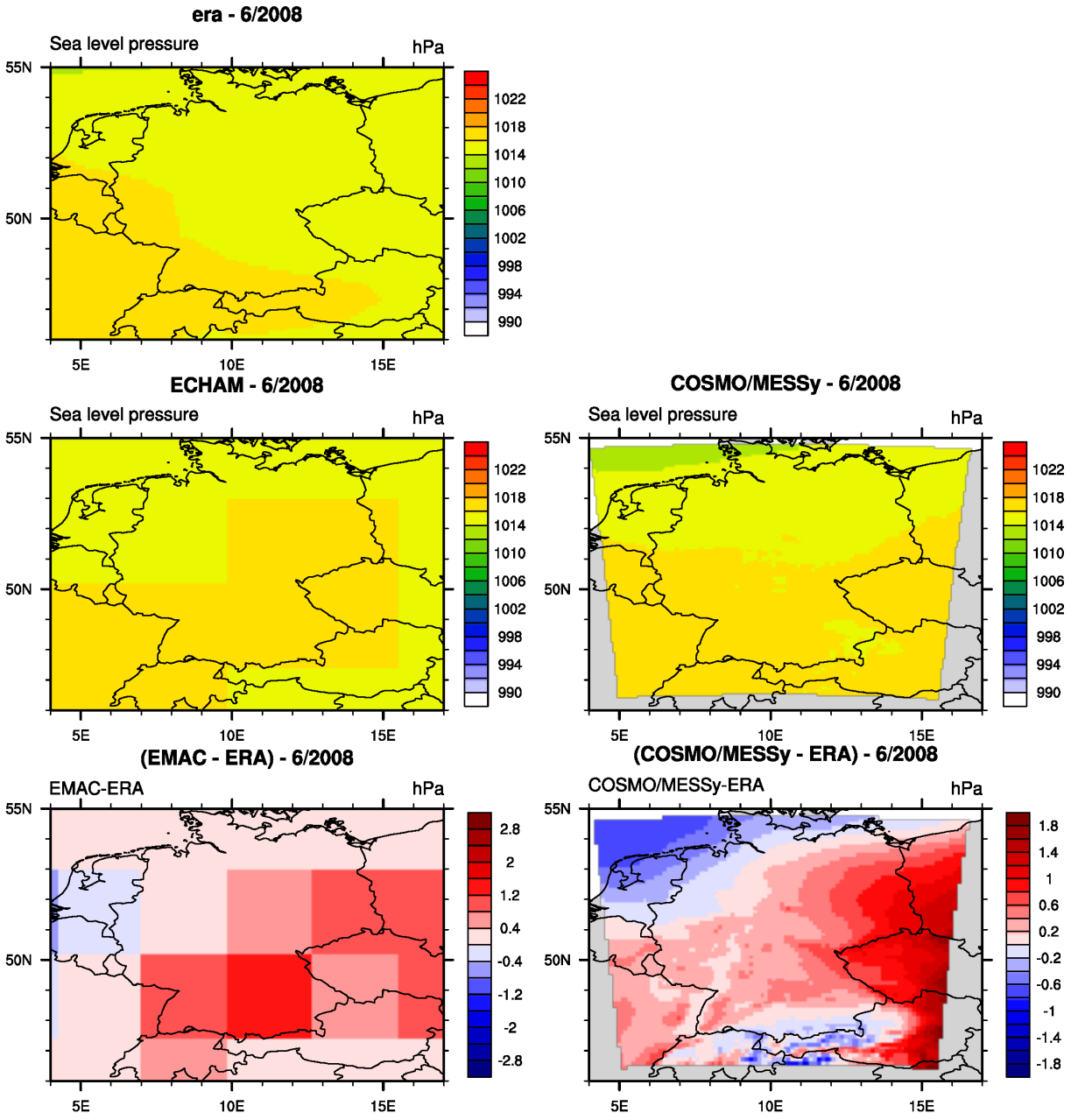

Figure S35: Comparison of the mean sea level pressure (in hPa) between EMAC, COSMO(12km)/MESSy and ERA Interim for June 2008. The upper three plots show the absolute values for ERA-Interim, EMAC and COSMO(12km)/MESSy. The lower row depicts the difference to ERA-Interim for EMAC (left) and COSMO(50km)/MESSy (right).

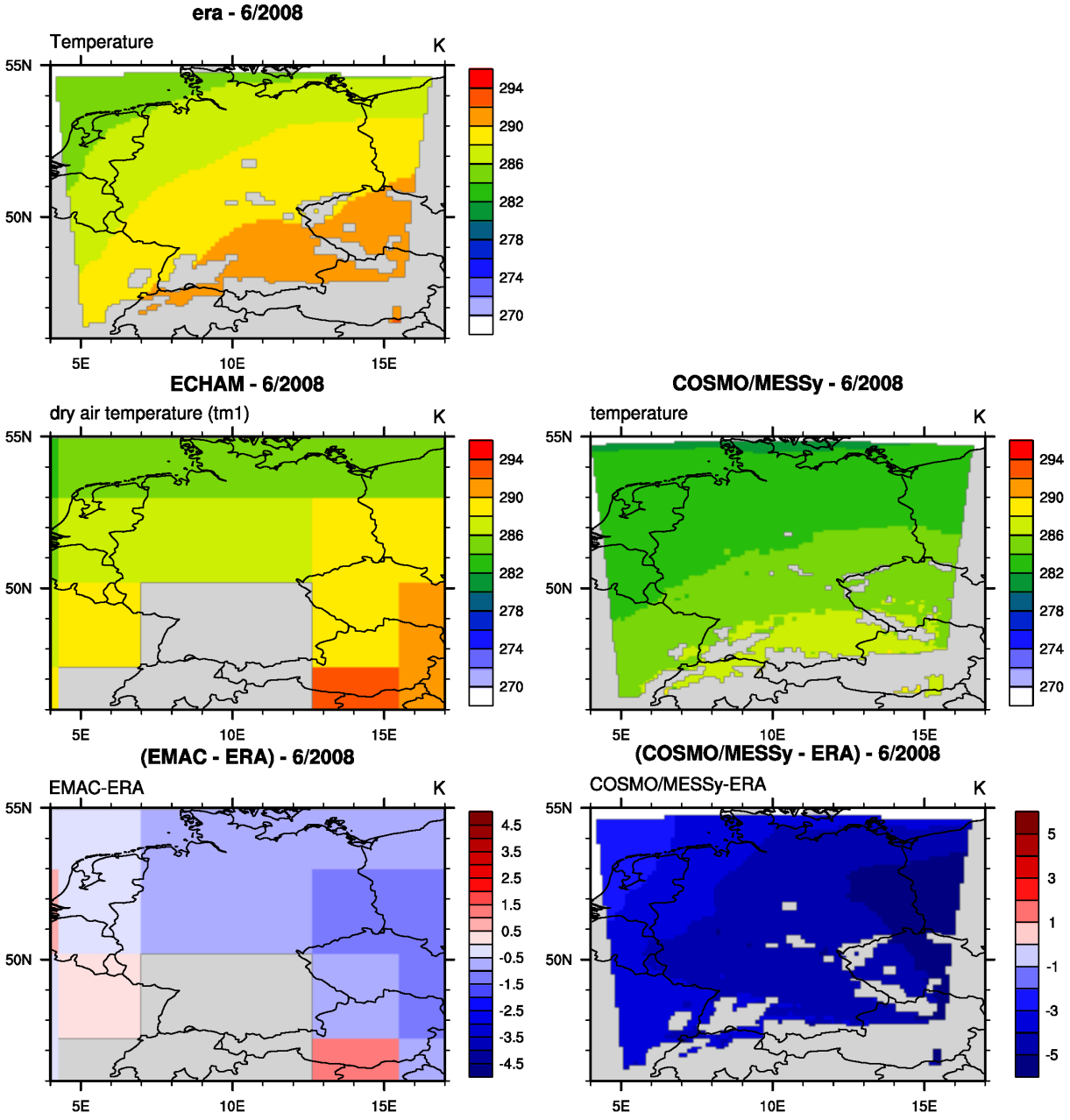

Figure S36: Comparison of the temperature at 950 hPa (in K) between EMAC, COSMO(12km)/MESSy and ERA Interim for June 2008. The upper three plots show the absolute values for ERA-Interim, EMAC and COSMO(12km)/MESSy. The lower row depicts the difference to ERA-Interim for EMAC (left) and COSMO(50km)/MESSy (right).

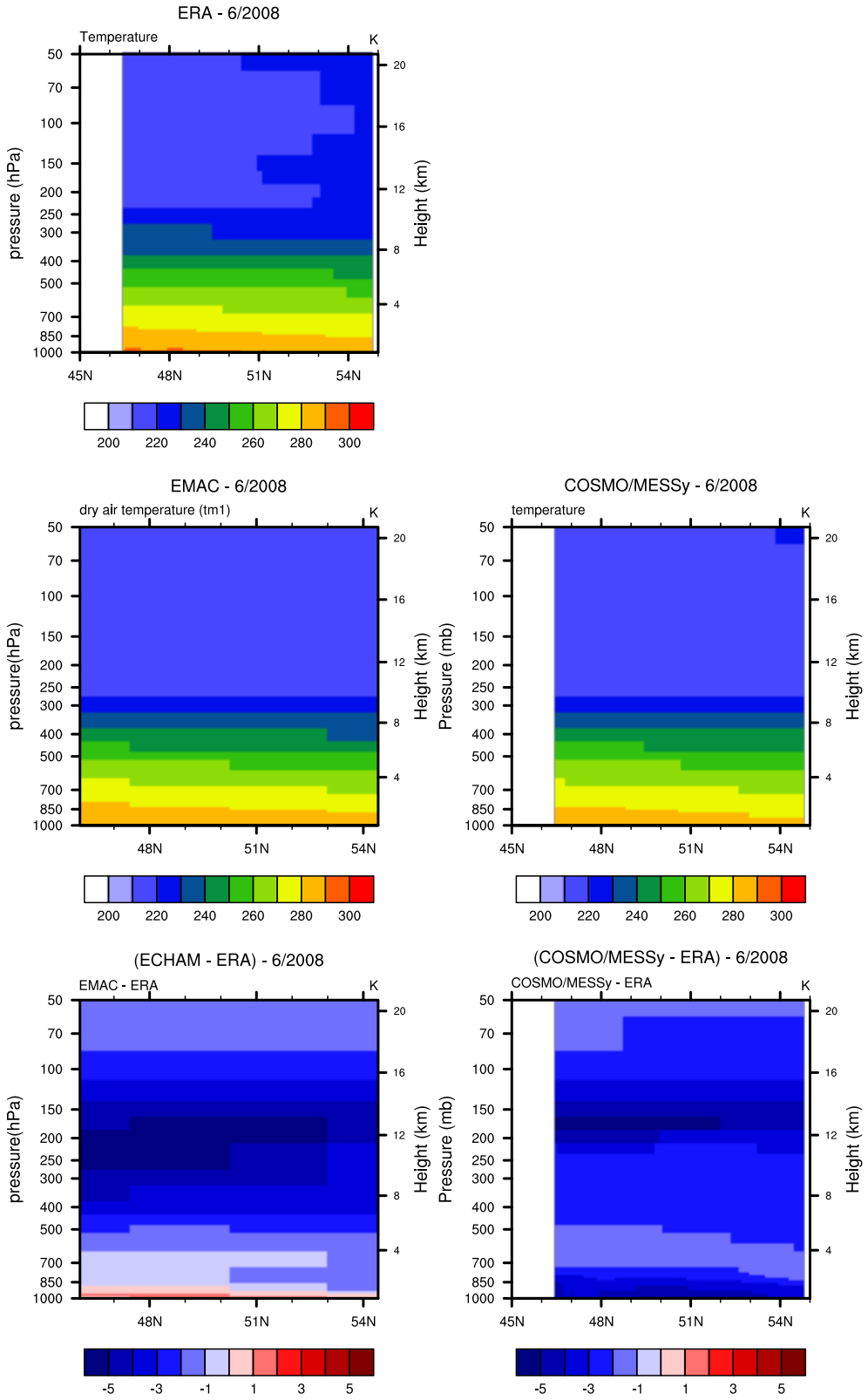

Figure S37: Comparison of zonal average temperature (in K) between EMAC, COSMO(12km)/MESSy and ERA Interim for June 2008. The upper three plots show the absolute values for ERA-Interim, EMAC and COSMO(12km)/MESSy. The lower row depicts the difference to ERA-Interim for EMAC (left) and COSMO(50km)/MESSy (right).

S3 Comparison with temperature profiles from ozone sondes

S3.1 COSMO(50km)/MESSy

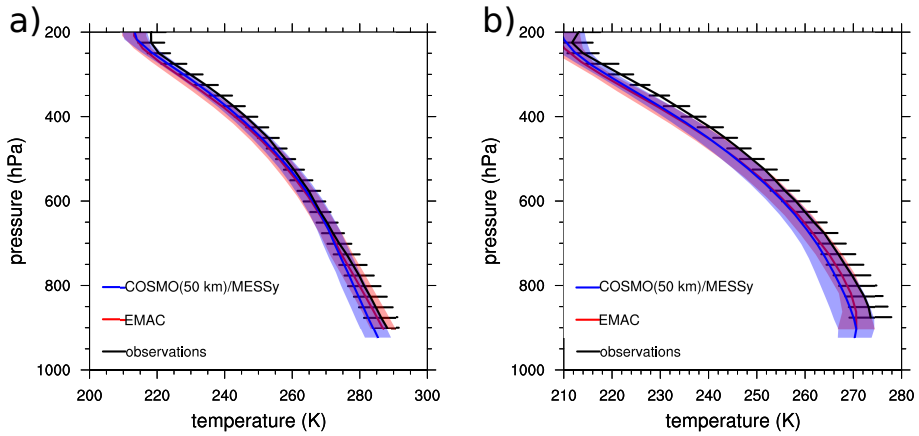

Figure S38: Vertical temperature profile at Hohenpeissenberg (in K) for **a)** June and **b)** December 2008. The standard deviation of the temporal mean is indicated by the error bars for the observations and by the shaded area for the model data.

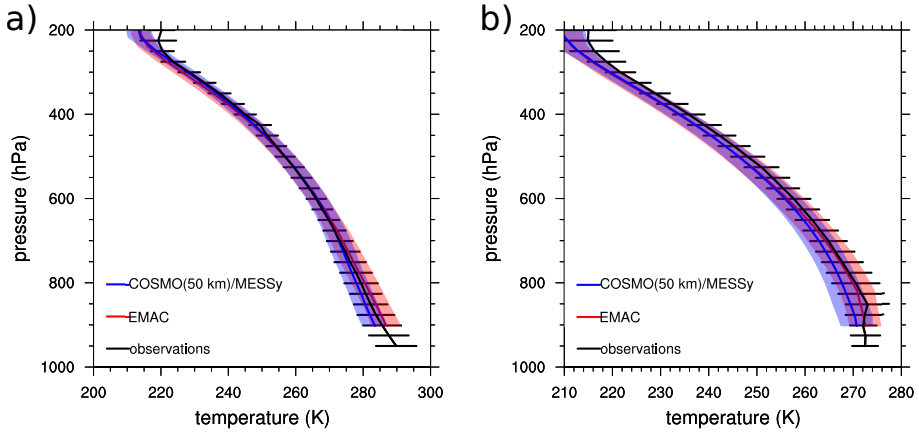

Figure S39: Vertical temperature profile at Payerne (in K) for (a) June and (b) December 2008. The standard deviation of the temporal mean is indicated by the error bars for the observations and by the shaded area for the model data.

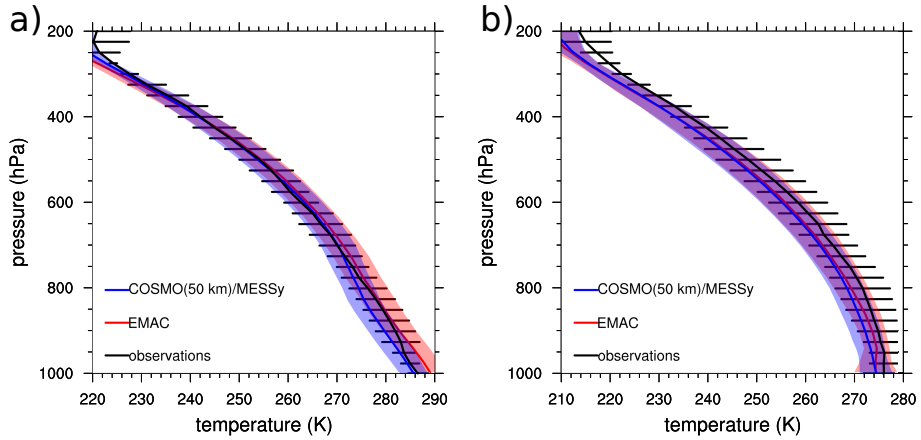

Figure S40: Vertical temperature profile at De Bilt (in K) for (a) June and (b) December 2008. The standard deviation of the temporal mean is indicated by the error bars for the observations and by the shaded area for the model data.

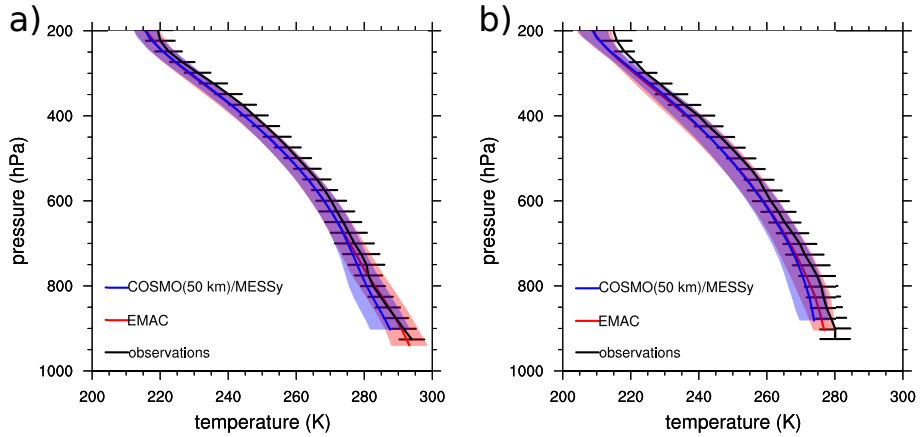

Figure S41: Vertical temperature profile at Madrid (in K) for (a) June and (b) December 2008. The standard deviation of the temporal mean is indicated by the error bars for the observations and by the shaded area for the model data.

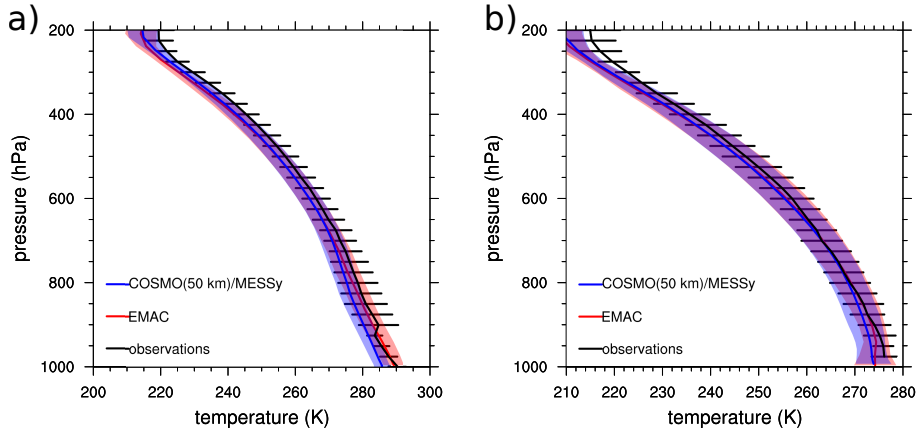

Figure S42: Vertical temperature profile at Uccle (in K) for (a) June and (b) December 2008. The standard deviation of the temporal mean is indicated by the error bars for the observations and by the shaded area for the model data.

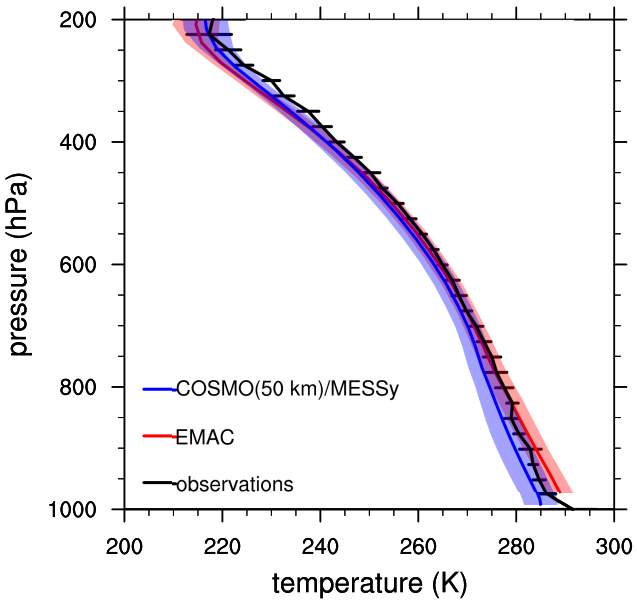

Figure S43: Vertical temperature profile at Legionowo for June 2008. The standard deviation of the temporal mean is indicated by the error bars for the observations and by the shaded area for the model data.

S4 COSMO-Namelists

The section shows a comparison between the COSMO namelists used in this study and the COSMO-CLM namelists for the simulations within the EURO CORDEX framework (12). Please note that this study uses a newer version of COSMO-CLM compared to the simulations described by (12), therefore some new namelist options are now available or defaults have been changed.

S4.1 'lmgrid'-namelist

Table S1: Comparison between the COSMO-lmgrid namelist used in this study and the CORDEX-EU COSMO-CLM namelist (please note that the namelist for CORDEX-EU is from the COSMO-CLM version 4.8-clm17, while we use COSMO 5.0, therefore some options are not available in COSMO 4.8-clm17 (marked with $*$)).

Variable	COSMO(50km)/MESSy	COSMO(12km)/MESSy	CORDEX-EU
pollon	-170	-170	-162
pollat	40	41	39.25
polgam	0	0	0
dlon	0.44	0.1	0.44
dlat	0.44	0.1	0.44
startlon_tot	-3.9	-25.6	-33.93
startlat_tot	-4.9	-27.6	-28.93
ie_tot	132	104	132
je_tot	122	114	129
ke_tot	40	40	40

S4.2 'runctl'-namelist

Table S2: Comparison between the COSMO-runcontrol namelist used in this study and the CORDEX-EU COSMO-CLM namelist (please note that the namelist for CORDEX-EU is from the COSMO-CLM version 4.8-clm17, while we use COSMO 5.0, therefore some options are not available (marked with $*$)).

Variable	COSMO(50km)/MESSy	COSMO(12km)/MESSy	CORDEX-EU
dt	240	120	300
itype_calendar	0	0	0
hincmxt	6	6	24
hincmxu	1	1	24
leps	F	F	F
lphys	T	T	T
ldiagnos	T	T	T
ldfi	F	F	F
luseobs	F	F	F
luse_rttov	F	F	F
l_cosmo_art	F	F	*
l_pollen	F	F	*
ldump_ascii	T	T	F
lreproduce	T	T	T
lreorder	F	F	F
lartif_data	F	F	F
lperi_x	F	F	*
lperi_y	F	F	*
l2dim	F	F	F
lroutine	F	F	*
llm	F	F	F
nprocx	12	20	16
nprocy	16	16	16
nprocio	0	0	0
num_asynio_comm	0	0	*
num_iope_percomm	0	0	*
nboundlines	3	3	3
ncomm_type	1	1	3
ldatatypes	F	F	F
ltime_barrier	T	T	F
itype_timing	4	4	4
idbg_level	10	10	2
ldebug_dyn	F	F	F
ldebug_gsp	F	F	F
ldebug_rad	F	F	F
ldebug_tur	F	F	F
ldebug_con	F	F	F
ldebug_soi	F	F	F
ldebug_io	F	F	F
ldebug_mpe	F	F	F
ldebug_dia	F	F	F
ldebug_art	F	F	F
ldebug_ass	F	F	F
ldebug_lhn	F	F	F

Continued on next page

Table S2 – *Continued from previous page*

Variable	COSMO(50km)/MESSy	COSMO(12km)/MESSy	CORDEX-EU
lprintdeb_all	F	F	F
linit_fields	F	F	F

S4.3 'tuning'-namelist

Table S3: Comparison between the COSMO-tuning namelist used in this study and the CORDEX-EU COSMO-CLM namelist (please note that the namelist for CORDEX-EU is from the COSMO-CLM version 4.8 -clm17, while we use COSMO 5.0, therefore some options are not available (marked with $*$)).

Variable	COSMO(50km)/MESSy	COSMO(12km)/MESSy	CORDEX-EU
crsmin	150	150	150
rat_lam	1	1	1
tkesmot	0,15	0,15	0,15
wichfakt	0,15	0,15	0
securi	0,5	0,5	0,85
tkhmin	1	1	1
tkmmin	1	1	1
rlam_mom	0	0	0
rlam_heat	1	1	1
rat_sea	20	20	20
rat_can	1	1	1
c_lnd	2	2	2
c_sea	1,5	1,5	1,5
c_soil	1	1	1
e_surf	1	1	1
pat_len	500	500	500
tur_len	500	500	500
z0m_dia	0,2	0,2	0,2
a_heat	0,74	0,74	0,74
a_mom	0,92	0,92	0,92
d_heat	10,1	10,1	10,1
d_mom	16,6	16,6	16,6
c_diff	0,2	0,2	0,2
a_hshr	0,2	0,2	*
a_stab	0	0	*
clc_diag	0,5	0,5	0,5
q_crit	4	4	4
qc0	0	0	0
qi0	0	0	0
gkdrag	0,075	0,075	0,075
gkwake	0,5	0,5	0,5
mu_rain	0	0,5	0,5
rain_n0_factor	1	1	*
v0snow	25	25	25
cloud_num	500000000	500000000	500000000
entr_sc	0,0003	0,0003	0,0003
thick_sc	25000	25000	*

S4.4 'dyncontrol'-namelist

Table S4: Comparison between the COSMO-dyncontrol namelist used in this study and the CORDEX-EU COSMO-CLM namelist (please note that the namelist for CORDEX-EU is from the COSMO-CLM version 4.8-clm17, while we use COSMO 5.0, therefore some options are not available (marked with ∗)).

Variable	COSMO(50km)/MESSy	COSMO(12km)/MESSy	CORDEX-EU
epsass	0,15	0,15	0,15
alphaass	1	1	0,53
betasw	0,4	0,4	0,4
betagw	0,4	0,4	0,4
beta2sw	0,4	0,4	0,4
beta2gw	0,4	0,4	0,4
lrubc	F	F	F
lspubc	T	T	T
lexpl_lbc	T	T	T
lradlbc	F	F	F
lcond	T	T	T
ldiabf_lh	T	T	T
lw_freeslip	T	T	T
l2tls	T	T	T
y_vert_adv_dyn	impl2	impl2	*
lsemi_imp	F	F	F
lhordiff	T	T	*
ldyn_bbc	F	F	T
lcori	T	T	T
lmetr	T	T	T
lcori_deep	F	F	F
ladv_deep	F	F	F
y_scalar_advect	BOTT2	BOTT2	BOTT2
rdheight	11000	11000	11000
crltau	1	1	1
rlwidth	700000	150000	500000
relax_fac	0,01	0,01	0,01
nrdtau	6	6	6
maxit_si	200	200	200
ikrylow_si	20	20	20
iprint_si	0	0	0
irunge_kutta	1	1	1
irk_order	3	3	3
iadv_order	5	5	3
ieva_order	3	3	3
itheta_adv	0	0	0
ltadv_limiter	F	F	*
itype_bbc_w	1	1	*
intcr_max	1	1	1
itype_outflow_qrsg	1	1	1
itype_lbc_qrsg	1	1	1
itype_spubc	1	1	1
nfi_spubc2	10	10	10
itype_hdiff	2	2	2

Continued on next page

Table S4 – *Continued from previous page*

Variable	COSMO(50km)/MESSy	COSMO(12km)/MESSy	CORDEX-EU
l_diff_Smag	T	T	*
hd_corr_u_bd	0	0	0.25
hd_corr_t_bd	0	0	*
hd_corr_trcr_bd	0	0	*
hd_corr_p_bd	0	0	*
hd_corr_u_in	0	0	*
hd_corr_t_in	0	0	*
hd_corr_trcr_in	0	0	*
hd_corr_p_in	0	0	*
hd_dhmax	250	250	250
xkd	0,1	0,1	0,1
divdamp_slope	20	20	*
eps_si	0	0	0
itype_fast_waves	1	1	*
lspecnudge	F	F	F

S4.5 'phycontrol'-namelist

Table S5: Comparison between the COSMO-phycontrol namelist used in this study and the CORDEX-EU COSMO-CLM namelist (please note that the namelist for CORDEX-EU is from the COSMO-CLM version 4.8 -clm17, while we use COSMO 5.0, therefore some options are not available (marked with $*$)).

Variable	COSMO(50km)/MESSy	COSMO(12km)/MESSy	CORDEX-EU
lgsp	T	T	T
ldiniprec	T	T	F
lrad	T	T	T
itype_aerosol	1	1	*
lemiss	F	F	*
lforest	F	F	T
ltur	T	T	T
l3dturb	F	F	F
l3dturb_metr	T	T	T
lprog_tke	F	F	F
limpltkediff	T	T	*
lconv	T	T	T
itype_conv	0	0	0
lconv_inst	F	F	F
lsoil	T	T	T
lseaice	F	F	*
llake	F	F	F
lsso	T	T	T
lmelt	T	T	T
lmelt_var	T	T	T
lmulti_layer	T	T	T
ke_soil	7	7	9
czbot_w_so	4	4	9
lturhor	F	F	F
lexpcor	F	F	F
ltmpcor	F	F	F
lprfcor	F	F	F
lnonloc	F	F	F
lcpfluc	F	F	F
lconf_avg	T	T	T
lradf_avg	F	F	F
lcape	F	F	F
lctke	F	F	F
hincrad	1	1	1
3 nincrad	12	12	12
nradcoarse	1	1	1
ninctura	1	1	1
nincconv	1	1	1
nincsso	5	5	5
itype_trvg	2	2	2
itype_evsl	2	2	2
itype_gscp	3	3	
itype_wcld	2	2	2
itype_tran	2	2	2

Continued on next page

Table S5 – *Continued from previous page*

Variable	COSMO(50km)/MESSy	COSMO(12km)/MESSy	CORDEX-EU
itype_turb	3	3	3
itype_synd	2	2	2
imode_tran	1	1	1
imode_turb	1	1	1
ico2_rad	8	8	8
iy_co2_stab	2001	2001	2001
lco2_stab	F	F	F
icldm_rad	4	4	4
icldm_tran	0	0	0
icldm_turb	2	2	2
nlgw	2	2	2
lradtopo	F	F	F
nhori	24	24	24
itype_albedo	2	2	2

S5 List of used stations

Table S6: Overview of stations from the EMEP network used for the comparison. The last column shows for which variables the station data were used.

Name	lat (in °)	lon (in °)	height (in m)	variable
Aliartos	38.37	23.08	110	O3, NO2
Anholt	56.71	11.51	40	NO2
Aston Hill	52.50	-3.03	370	NO2
Auchencorth Moss	55.79	-3.24	260	HNO3
Ayia Marina	35.04	33.06	532	O3
Barcorotta	38.48	-6.92	393	O3, NO2
Birkesens	58.38	8.25	190	O3,NO2, HNO3
Cabau Ziideweg	51.97	4.93	1	NO2
Campisabalos	41.28	-3.14	1360	C5H8
Chopok	48.93	19.58	2008	NO2, HNO3
Dezi	52.30	4.50	4	NO2
Diabla Gora	54.15	22.07	157	HNO3
Els Torms	41.40	0.72	470	NO2
Eskdalemuir	51.57	-3.20	243	NO2
Eupen	50.63	6.00	295	O3, NO2
Forsthof	48.11	15.92	581	O3
Giordon Lighthouse	36.07	14.22	167	O3
Graz Platte	47.11	15.47	651	O3
Harwell	51.57	-13.16	137	NO2
Hoburgen	56.91	18.15	58	NO2
Hurdal	60.37	11.08	300	HNO3
Illmitz	47.76	16.76	117	CO,NO2,HNO3
Iskraba	45.57	14.87	520	O3,NO2
Ispra	45.80	8.63	209	O3,NO2
Jarczew	51.82	21.98	180	O3,NO2
Jungfraujoch	46.54	7.98	3578	O3,CO, NO2
Keldsnor	54.73	10.73	10	NO2
Kollumerwaard	53.33	6.28	1	CO
Kosetice	49.58	15.08	535	NO2,CO,C5H8
Krvavec	46.30	14.54	1740	CO,HNO3
La Coulande	48.63	-0.45	304	O3
La Tardiere	46.65	-0.75	133	NO2
Ladybower Research	53.40	-1.75	420	O3,NO2
Lahemaa	59.50	25.90	32	O3
Lazaropole	41.54	20.69	1332	O3
Le Casset	45.00	6.47	1790	O3
Leova II	46.48	28.28	166	HNO3
Lullington Heathrow	50.79	0.18	120	O3,NO2
Mace Head	53.17	-9.50	15	O3
Montellipreti	42.10	12.63	48	O3,NO2, HNO3
Narberth	51.78	-4.69	160	NO2
Neuglobsow	53.17	13.03	62	O3,NO2, HNO3, C5H8
Niembro	43.44	-4.85	134	O3, NO2
Noraa-Kvill	57.82	15.57	261	O3
O Saviñao	43.23	-7.70	506	NO2
St. Osyth	51.78	1.08	8	CO,NO2

Continued on next page

Table S6 – *Continued from previous page*

Name	lat (in °)	lon (in °)	height (in m)	variable
Pallas	68.0	24.15	340	C5H8
Penausende	41.28	-5.87	985	NO2
Peyrusse Vieille	43.62	0.19	200	C5H8, NO2
Pic du Midi	42.94	0.14	2887	O3
Preila	55.35	21.06	5	O3,NO2
Puy de Dome	45.77	2.95	1468	O3,CO
Revin	49.90	4.63	390	O3, HNO3
Rigi	47.07	8.46	1031	HNO3, C5H8
Rojen Peak	41.70	24.74	1750	O3
Rucava	56.16	21.17	18	O3
Schauinsland	47.92	7.92	1205	O3,CO, NO2, HNO3, C5H8
Schmücke	50.65	10.77	937	O3, NO2, C5H8
Søgne	58.11	7.85	15	HNO3
Sniezka	50.73	15.73	16	NO2
Sonnblick	47.05	12.96	3106	CO
Starina	49.05	22.27	345	O3,NO2, HNO3, C5H8
Sulzberg	47.53	9.93	1020	O3
Svratouch	49.83	16.05	737	NO2
La Tardiàre	46.65	-0.75	133	C5H8
Tustervatn	65.83	13.91	439	HNO3
Ulborg	56.28	8.43	10	O3
Vilsandi	58.38	21.81	6	O3
Vizna	37.23	-3.53	1296	O3, NO2
Vorhegg	46.62	12.97	1020	CO,NO2
Vredepel	51.54	5.85	28	NO2
Waldhof	52.80	10.75	74	O3, NO2, HNO3, C5H8
Westerland	54.93	8.31	12	O3, NO2, HNO3
Zarra	39.09	-1.10	885	NO2
Zingst	54.43	12.73	1	O3, NO2, HNO3, O3, NO2, C5H8, HNO3
Zoesni	57.14	25.91	188	O3, NO2, C5H8

Table S7: Overview of stations providing vertical ozone profiles used for comparison. The last column shows for which variables the station data were used.

Name	lat (in °)	lon (in °)	height (in m)	variable
De Bilt	52.10	5.18 E	2	O3
Hohenpeisenberg	47.80	11.01	985	O3, C5H8
Leginowo	52.40	29.97	96	O3
Madrid	40.45	3.72	680	O3
Payerne	46.81	6.94	490	O3
Uccle	50.80	4.36	100	O3
Valentia	51.94	10.25	14	O3

S6 Detailed list of used submodels

Table S8: Overview of the submodels running in EMAC and COSMO/MESSy respectively. Both COSMO/MESSy instances use the same submodels.

Submodel	EMAC	COSMO	short description	references
AEROPT	x		calculation of aerosol optical properties	(1)
AIRSEA	x	x	exchange of tracers between air and sea	(14)
CH4	x		methane oxidation and feedback to hydrological cycle	
CLOUD	x		cloud parametrisation	(16), (7)
CLOUDOPT	x		cloud optical properties	
CONVECT	x		convection parametrisation	(19)
CVTRANS	x	x	convective tracer transport	(21)
DRADON	x	x	emission and decay of ^{222}Radon	(6)
DDEP	x	x	dry deposition of aerosols and tracer	(9)
E2COSMO	x		additional ECHAM5 fields for COSMO coupling	(10)
GWAVE	x		parametrisation of non-orographic gravity waves	(15)
H2O	x		stratospheric water vapour and its feedback	(7)
JVAL	x	x	calculation of photolysis rates	(13), (7)
LNOX	x		NO_x-production by lighting	(20), (6)
MECCA	x	x	tropospheric and stratospheric gas-phase chemistry	(17), (6)
MMD*	x	x	coupling of EMAC and COSMO/MESSy (including libraries and all submodels)	(10)
MSBM	x	x	multiphase chemistry of the stratosphere	(6)
O3ORIG	x		ozone origin diagnostics	(3)
OFFEMIS	x	x	prescribed emissions of trace gases and aerosols	(11)
ONEMIS	x	x	on-line calculated emissions of trace gases and aerosols	(11)
ORBIT	x	x	Earth orbit calculations	(1)
PTRAC	x	x	definition of prognostic tracers	(5)
QBO	x		Newtonian relaxation of the quasi-biennial oscillation (QBO)	(2), (7)
RAD	x		radiative transfer calculations calculation	(1)
S4D	x	x	diagnostic sampling along predefined tracks	(6)
SATSIMS	x		satellite simulator	
SCALC	x	x	simple calculations	(6)
SCAV	x	x	wet deposition and scavenging of trace gases and aerosols	(18)
SCOUT	x	x	diagnostic sampling at predefined locations	(6)
SEDI	x	x	sedimentation of aerosols	(9)
SORBIT	x	x	sampling along sun synchronous satellite orbits	(6)
SURFACE	x		surface properties	(8)
TAGGING	x	x	TAGGING of source attributions	(4)
TBUDGET	x		contribution of processes to a tracer	(8)

Continued on next page

Table S8 – *Continued from previous page*

Submodel	EMAC	COSMO	short description	references
TNUDGE	x	x	Newtonian relaxation of tracers	(11)
TREXP	x		emission of tracers at point sources	(6)
TROPOP	x	x	diagnostic calculation of tropopause height and additional diagnostics	(7)
VISO	x	x	sampling on isosurfaces	(6)

S7 References

References

[1] Dietmüller et. al. in preperation. *GMDD*, 2015.

[2] Marco A. Giorgetta and Lennart Bengtsson. Potential role of the quasi-biennial oscillation in the stratosphere-troposphere exchange as found in water vapor in general circulation model experiments. *Journal of Geophysical Research: Atmospheres*, 104(D6):6003–6019, 1999.

[3] V. Grewe. The origin of ozone. *Atmospheric Chemistry and Physics*, 6(6):1495–1511, 2006.

[4] Grewe et al. in preperation. *GMDD*, 2016.

[5] P. Jöckel, A. Kerkweg, J. Buchholz-Dietsch, H. Tost, R. Sander, and A. Pozzer. Technical note: Coupling of chemical processes with the modular earth submodel system (messy) submodel tracer. *Atmospheric Chemistry and Physics*, 8(6):1677–1687, 2008.

[6] P. Jöckel, A. Kerkweg, A. Pozzer, R. Sander, H. Tost, H. Riede, A. Baumgaertner, S. Gromov, and B. Kern. Development cycle 2 of the modular earth submodel system (messy2). *Geoscientific Model Development*, 3(2):717–752, 2010.

[7] P. Jöckel, H. Tost, A. Pozzer, C. Brühl, J. Buchholz, L. Ganzeveld, P. Hoor, A. Kerkweg, M. G. Lawrence, R. Sander, B. Steil, G. Stiller, M. Tanarhte, D. Taraborrelli, J. van Aardenne, and J. Lelieveld. The atmospheric chemistry general circulation model echam5/messy1: consistent simulation of ozone from the surface to the mesosphere. *Atmospheric Chemistry and Physics*, 6(12):5067–5104, 2006.

[8] P. Jöckel, H. Tost, A. Pozzer, M. Kunze, O. Kirner, C. A. M. Brenninkmeijer, S. Brinkop, D. S. Cai, C. Dyroff, J. Eckstein, F. Frank, H. Garny, K.-D. Gottschaldt, P. Graf, V. Grewe, A. Kerkweg, B. Kern, S. Matthes, M. Mertens, S. Meul, M. Neumaier, M. Nützel, S. Oberländer-Hayn, R. Ruhnke, T. Runde, R. Sander, D. Scharffe, and A. Zahn. Earth system chemistry integrated modelling (escimo) with the modular earth submodel system (messy, version 2.51). *Geoscientific Model Development Discussions*, 8(10):8635–8750, 2015.

[9] A. Kerkweg, J. Buchholz, L. Ganzeveld, A. Pozzer, H. Tost, and P. Jöckel. Technical note: An implementation of the dry removal processes dry deposition and sedimentation in the modular earth submodel system (messy). *Atmospheric Chemistry and Physics*, 6(12):4617–4632, 2006.

[10] A. Kerkweg and P. Jöckel. The 1-way on-line coupled atmospheric chemistry model system meco(n) - part 2: On-line coupling with the multi-model-driver (mmd). *Geoscientific Model Development*, 5(1):111–128, 2012.

[11] A. Kerkweg, R. Sander, H. Tost, and P. Jöckel. Technical note: Implementation of prescribed (offlem), calculated (onlem), and pseudo-emissions (tnudge) of chemical species in the modular earth submodel system (messy). *Atmospheric Chemistry and Physics*, 6(11):3603–3609, 2006.

[12] S. Kotlarski, K. Keuler, O. B. Christensen, A. Colette, M. Déqué, A. Gobiet, K. Goergen, D. Jacob, D. Lüthi, E. van Meijgaard, G. Nikulin, C. Schär, C. Teichmann, R. Vautard, K. Warrach-Sagi, and V. Wulfmeyer. Regional climate modeling on european scales: a joint standard evaluation of the euro-cordex rcm ensemble. *Geoscientific Model Development*, 7(4):1297–1333, 2014.

[13] J. Landgraf and P. J. Crutzen. An efficient method for online calculations of photolysis and heating rates. *J. Atmos. Sci.*, 55:863–878, 1998.

[14] A. Pozzer, P. Jöckel, R. Sander, J. Williams, L. Ganzeveld, and J. Lelieveld. Technical note: The messy-submodel airsea calculating the air-sea exchange of chemical species. *Atmospheric Chemistry and Physics*, 6(12):5435–5444, 2006.

[15] E. Roeckner, G. Bäuml, L. Bonaventura, R. Brokopf, M. Esch, M. Giorgetta, S. Hagemann, I. Kirchner, L. Kornblueh, E. Manzini, A. Rhodin, U. Schlese, U. Schulzweida, and A. Tompkins. The atmospheric general circulation model echam5. part i: Model description. MPI-Report 349, Max Planck Institut für Meteorologie in Hamburg, Deutschland, 2003. available at:

https://www.mpimet.mpg.de/fileadmin/publikationen/Reports/max_scirep_349.pdf (last access: 18 October 2015).

[16] E. Roeckner, R. Brokopf, M. Esch, M. Giorgetta, S. Hagemann, L. Kornblueh, E. Manzini, U. Schlese, and U. Schulzweida. Sensitivity of Simulated Climate to Horizontal and Vertical Resolution in the ECHAM5 Atmosphere Model. *J. Climate*, 19(16):3771–3791, August 2006.

[17] R. Sander, A. Baumgaertner, S. Gromov, H. Harder, P. Jöckel, A. Kerkweg, D. Kubistin, E. Regelin, H. Riede, A. Sandu, D. Taraborrelli, H. Tost, and Z.-Q. Xie. The atmospheric chemistry box model caaba/mecca-3.0. *Geoscientific Model Development*, 4(2):373–380, 2011.

[18] H. Tost, P. Jöckel, A. Kerkweg, R. Sander, and J. Lelieveld. Technical note: A new comprehensive scavenging submodel for global atmospheric chemistry modelling. *Atmospheric Chemistry and Physics*, 6(3):565–574, 2006.

[19] H. Tost, P. Jöckel, and J. Lelieveld. Influence of different convection parameterisations in a gcm. *Atmospheric Chemistry and Physics*, 6(12):5475–5493, 2006.

[20] H. Tost, P. Jöckel, and J. Lelieveld. Lightning and convection parameterisations – uncertainties in global modelling. *Atmospheric Chemistry and Physics*, 7(17):4553–4568, 2007.

[21] H. Tost, M. G. Lawrence, C. Brühl, P. Jöckel, The GABRIEL Team, and The SCOUT-O3-DARWIN/ACTIVE Team. Uncertainties in atmospheric chemistry modelling due to convection parameterisations and subsequent scavenging. *Atmospheric Chemistry and Physics*, 10(4):1931–1951, 2010.